A computer model of laser action in the teaching of computational physics

D. G. H. Andrews, and D. R. Tilley

Citation: American Journal of Physics **59**, 536 (1991); doi: 10.1119/1.16815
View online: https://doi.org/10.1119/1.16815
View Table of Contents: http://aapt.scitation.org/toc/ajp/59/6
Published by the American Association of Physics Teachers

A computer model of laser action in the teaching of computational physics

D. G. H. Andrews[a] and D. R. Tilley
University of Essex, Colchester CO4 3SQ, Essex, United Kingdom

(Received 10 July 1990; accepted for publication 28 November 1990)

An undergraduate computational project is described. A set of rate equations for a four-level laser is presented. The steady-state equations are solved exactly to find nonlasing and lasing solutions and the critical pump rate for the transition between them. The steady-state solutions are used as a guide to the introduction of suitable dimensionless variables for the rate equations. Illustrative numerical solutions of the rate equations in dimensionless form are presented. The detailed account given of this example is used to bring out a number of points about teaching computational physics.

I. INTRODUCTION

Computers are now a common feature of physics degree courses.[1] They are often used as teaching aids, and also students are usually taught a certain amount of computational physics. At a more elementary level, students may be presented with prewritten programs for physical processes which they can investigate, for example, by manipulating the initial conditions. At an advanced level, however, it is more instructive if students are given a model, typically a mathematical description of a physical system, and asked to explore its properties by a combination of analytic and numerical methods, which is characteristic of much of computational physics. In this paper we describe an example of this kind of modeling, which was originally set as a final year computing project in the Physics Department of the University of Essex. A brief account is given as example 3 of Tilley.[1] We give a fuller account here first to describe in somewhat more detail the physics of a simple laser model and to bring out something of the interplay between analytical study, numerical study, and physical insight that is needed for a thorough understanding, and second to make some general points about teaching computational physics. These general points are left to the final section.

The problem involves the modeling of rate equations for a simpler laser. These equations determine the number densities of the atoms in the appropriate energy levels and the average energy density within the laser cavity. The project illustrates the physical processes occurring within the laser and also the techniques needed to solve physical equations numerically. As a first step, the steady-state equations are obtained from the differential rate equations for the laser. These can be solved analytically and give the physical conditions necessary for lasing. The rate equations can then be scaled in units of the steady-state values, which gives a formulation in terms of dimensionless variables. Such a scaling is necessary before the rate equations can be handled numerically, and indeed the example brings out clearly the point that there is a good deal of analytical work to be done before the numerical work begins.

Our students had taken a course on FORTRAN in the previous year and, therefore, carried out the modeling by constructing FORTRAN programs. With the availability of extensive subroutine libraries, such as those of NAG,[2] IMSL, or Press *et al.*,[3] there is no obvious advantage to be gained from physics students writing their own subroutines for standard numerical processes like the integration of ordinary differential equations, although it is clearly important that they understand enough to become discerning customers. For example, it will be seen that the action of our laser involves two very different time scales, so that the student should be aware that the differential equations may suffer from the complicating feature of "stiffness," although it emerges that they do not. In practice, the graphs we present were obtained with a variable-step-length fourth-order Runge–Kutta subroutine from Press *et al.*,[4] whereas the students used a variant known as Runge–Kutta–Merson from the NAG Library.[2] No significant practical difference was found between the two subroutines.

Clearly, graphics output is an enormous benefit in work of this kind. Some years ago, graphics had to be obtained by the relatively laborious technique of a sequence of subroutine calls, but nowadays the availability of spreadsheet-type graphics packages makes the task much easier. Simple-to-use graphics greatly facilitates carrying out numerical experiments, such as the buildup of energy within the cavity after the laser is switched on.

II. ANALYSIS

Lasers can be classified into three- and four-level lasers. The four-level laser will be analyzed, and an idealized model is shown in Fig. 1. Important examples of the four-level laser include Nd^{3+}-glass and CO_2 lasers. Atoms in the ground state are pumped into level 3 at rate R. Energy can be pumped into the laser medium in several ways, for example, by means of an electrical discharge. The atoms in level 3 decay rapidly and nonradiatively into level 2. The spontaneous decay from level 2 to 1 is slow, while that from level 1 to the ground state is rapid. This produces the possibility of a population inversion between levels 1 and 2, in which case stimulated emission predominates for the $2 \rightarrow 1$ transition. Light from this transition is confined within the laser medium with the cavity mirrors and is rapidly amplified. A small fraction of the light is allowed to escape through the partially transmitting mirror and this forms the intense laser beam.

A set of rate equations that describe this laser is as follows:

$$\frac{dN_1}{dT} = -\frac{N_1}{T_1} + A_{21}N_2 + B_{21}(N_2 - N_1)W, \tag{1}$$

$$\frac{dN_2}{dT} = R - A_{21}N_2 - B_{21}(N_2 - N_1)W, \tag{2}$$

$$\frac{dW}{dT} = hvg(v)\left[A'_{21}N_2 + B_{21}(N_2 - N_1)W\right] - \frac{W}{T_0}. \tag{3}$$

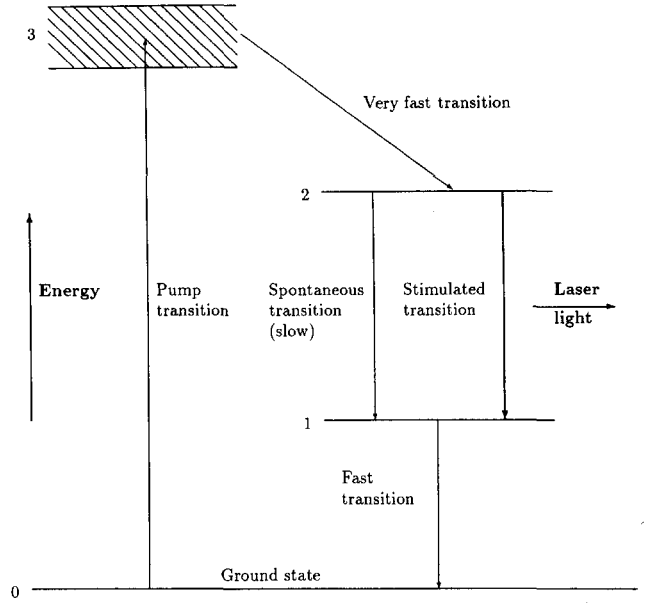

Fig. 1. Energy-level scheme for four-level laser.

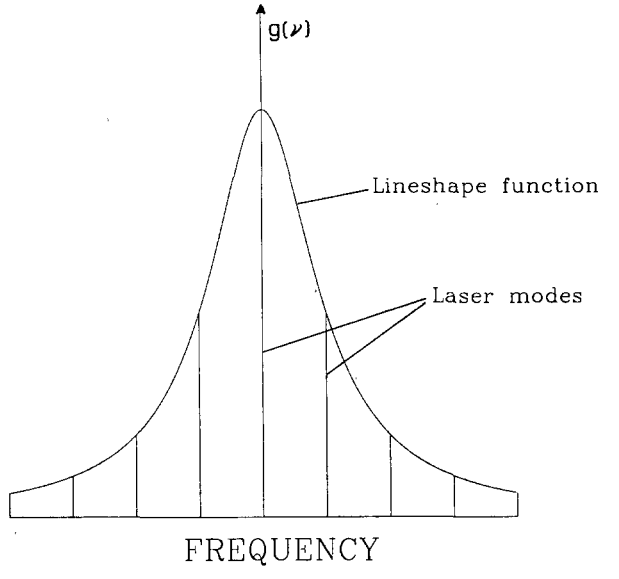

Fig. 2. Lorentzian line shape [Eq. (4)] as a function of frequency ν. Cavity modes of the laser are indicated for the case when mode spacing is less than the linewidth. In this paper, however, it is assumed that mode spacing is greater than the linewidth, and that the single mode of interest falls at the center of the line.

Equation (1) gives the rate of change of the average number density N_1 of atoms in level 1. The first term on the right-hand side gives the rate of decay of atoms from level 1 to the ground level with time constant T_1. The second term is the rate of spontaneous decay of atoms for the transition $2 \rightarrow 1$. A_{21} is the Einstein coefficient for spontaneous emission and is the inverse of the spontaneous time constant T_2 of level 2. The last term is the rate of stimulated transition between levels 2 and 1. The electromagnetic energy within the cavity per unit volume per unit frequency in the lasing mode is W. B_{21} is the Einstein coefficient for stimulated emission; it is related to A_{21} by the equation $A_{21}/B_{21} = 8\pi h\nu^3/c^3$, where h is Planck's constant, ν is the frequency, and c is the velocity of light.

Equation (2) gives the rate of change of the average number density of atoms in level 2. The first term on the right-hand side is the pump rate R, since it is assumed that all atoms in level 3 rapidly decay into level 2. The other terms are the same as those in Eq. (1), but with the opposite sign.

Equation (3) gives the rate of change of energy within the cavity in the lasing mode. Within the square brackets is the rate of stimulated decay between levels 2 and 1, together with the term $A'_{21}N_2$, which is the spontaneous decay rate into the lasing mode. These terms give the rate of change of energy density in photon numbers; they are multiplied by the photon energy $h\nu$ and a line-shape function $g(\nu)$ of dimension ν^{-1}. The last term is the rate of loss of energy from the cavity. The photon lifetime within the cavity is T_0, which is determined by the reflectivity of the mirror and the cavity length, and also by the absorption and scattering of the photons.

These equations are the standard rate equations for a four-level laser (e.g., Yariv).[4] Spontaneous decay into the lasing mode produces the initial noise, which is amplified within the oscillator cavity. Other possible transitions have been neglected. The rate equation model can be derived from the more sophisticated density matrix model (e.g., Loudon[5]) by considering only the diagonal elements. If the off-diagonal elements are included, aspects of coherence are introduced. However, the rate equation model is usually taught at the undergraduate level and the underlying physics is sound, so that it is sufficient for this project.

The line-shape function $g(\nu)$ in (3) is the frequency distribution for the transition $2 \rightarrow 1$. The lifetime broadening has the normalized Lorentzian form

$$g(\nu) = \Delta\nu/2\pi[(\nu - \nu_0)^2 + (\Delta\nu/2)^2], \tag{4}$$

where $\Delta\nu$ is the linewidth and ν_0 is the center frequency. Within this natural emission line, there may be several modes in which the laser can operate, as shown in Fig. 2. For simplicity, however, it is assumed here that only a single, monochromatic lasing mode is present and that it is at the center frequency. The amplitude of the line is then

$$g(\nu_0) = 2/\pi\,\Delta\nu. \tag{5}$$

The width of the emission line is largely determined by the lifetime of the two levels:

$$\Delta\nu = (1/\pi T_1) + (1/\pi T_2). \tag{6}$$

Thus

$$g(\nu_0) = 2/[A_{21} + (1/T_1)]. \tag{7}$$

This value can be used in (3).

Any transition between levels 2 and 1 will produce light in the range of frequencies under the curve in Fig. 2. The spontaneous decay rate for all these transitions is A_{21}, while A'_{21} is the spontaneous decay rate for the transition into the center mode. This means that, in practice, the ratio A'_{21}/A_{21} is extremely small.

III. STEADY-STATE SOLUTIONS

The first step in studying the behavior of the laser is to find the steady-state conditions by equating the time derivatives to zero. These conditions will determine the behavior of a continuous-wave (cw) laser after the initial warm-up period. In order to simplify the analysis, the small term $A'_{21}N_2$ is neglected here.

The sum of (1) and (2) gives

$$N_1 = RT_1, \tag{8}$$

and (2) then expresses N_2 in terms of W:

$$N_2 = R(1 + B_{21} WT_1)/(A_{21} + B_{21} W). \tag{9}$$

Equation (3) then gives

$$W[(W/T_0) - h\nu g(\nu)R(1 - A_{21} T_1) + (A_{21}/B_{21} T_0)] = 0, \tag{10}$$

so that there are two possible solutions:

$$W = 0 \tag{11}$$

or

$$W = h\nu g(\nu)R(1 - A_{21} T_1)T_0 - (A_{21}/B_{21}). \tag{12}$$

Thus the system can have two possible states. The state described by (11) is not lasing, since there is no energy, while in (12) the energy can be greater than zero, and so the system is lasing. There will be a transition between the two states at a critical pump rate R_c. This transition is closely analogous to a phase transition in thermodynamics and, indeed, is usually referred to as a phase transition. Since the energy in (12) must be positive, the first term must be positive and greater than the second term. This determines the conditions for laser action, namely,

$$A_{21} T_1 < 1, \tag{13}$$

$$R > R_c = A_{21}/T_0 B_{21} h\nu g(\nu)(1 - A_{21} T_1). \tag{14}$$

The first condition means that $T_1 < T_2$; i.e., the decay from level 1 must be sufficiently rapid to maintain a population inversion. The second condition gives the critical pump rate R_c, which is necessary to achieve lasing. Above threshold, the relation between the pump rate and the energy output is linear. Also, above threshold the population inversion is

$$N_2 - N_1 = 8\pi\nu^2/A_{21} c^3 g(\nu) T_0, \tag{15}$$

which is constant. The steady-state solutions are shown in Fig. 3. Below the critical pump rate R_c, only the zero-power, nonlasing solution of (11) exists, and N_1 and N_2 increase linearly with R according to (8) and (9). For $R > R_c$, Fig. 3 shows only the lasing solution corresponding to (12), with (8) and (9). Within the lasing state, it can be seen that the slopes of (8) and (9) are identical as predicted by (15).

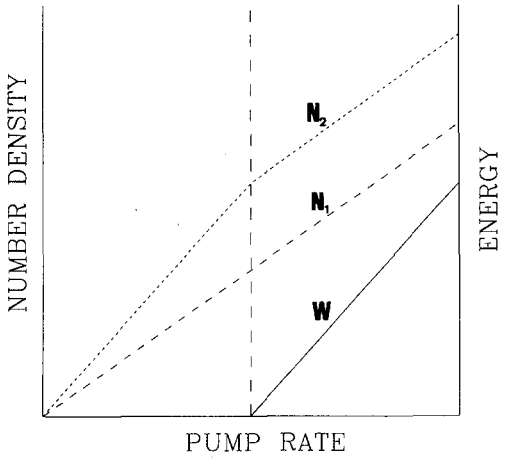

Fig. 3. Steady-state solutions of rate equations versus pump rate R.

It can be seen from (8)–(11) that the nonlasing solution persists for $R > R_c$. However, simple analysis shows that, in fact, it is unstable, in that any small perturbation leads to an increase in the energy W. To see this, we assume that the system is initially in the nonlasing state for $R > R_c$, and write $N_1 = RT_1 + \alpha_1$ and $N_2 = R/A_{21} + \alpha_2$, so that α_1 and α_2 are small deviations. The presence of α_1 and α_2 corresponds to a small energy density W in the cavity. Equation (3) for W now becomes

$$\frac{dW}{dT} = h\nu g(\nu) B_{21}\left(\frac{R}{A_{21}} - RT_1\right)W - \left(\frac{W}{T_0}\right), \tag{16}$$

where products such as $W\alpha_1$ have been neglected. It can be seen that for $W > 0$ the right-hand side of (16) is negative for $R < R_c$ and positive for $R > R_c$. Thus, for $R < R_c$, the energy decays toward zero after the perturbation, while for $R > R_c$ it continues to increase. As stated, the nonlasing solution is unstable for $R > R_c$.

For pump rates below threshold, the reintroduction of A'_{21} slightly modifies the above results. There is then a quadratic relation between the energy and pump rate, so that the nonlasing solution has nonzero energy, but this is very small compared to the energy in a typical lasing solution. The complexity of the solution when A'_{21} is included illustrates the importance of making approximations at the right point. In particular, A'_{21} cannot be neglected when solving the differential rate equations, since it is the spontaneous decay that produces the initial photons which are amplified to give laser light.

IV. NUMERICAL SOLUTION OF THE TIME-DEPENDENT EQUATIONS

In order to solve equations numerically, it is usually necessary to write them in terms of dimensionless variables. If this is not done, the numbers often become too large and produce numerical inaccuracy or even overflow. For instance, in this problem, N_1 and N_2 are of the order of 10^{23} m^{-3}.

In choosing dimensionless variables, it is logical to use the steady-state solutions. First, note that there are three time constants T_0, T_1, and T_2 so that there is a choice of time variables. The scaling $t = T/T_2 = A_{21} T$ was selected so that the dimensionless parameters $t_0 = A_{21} T_0$ and $t_1 = A_{21} T_1$ appear in the resulting equations.

The natural choice for scaling the pump rate R is the threshold value R_c, and so we define $r = R/R_c$. At threshold, $N_2 = N_c = R_c/A_{21}$, and so the number densities can be scaled to give $n_1 = N_1/N_c$ and $n_2 = N_2/N_c$. Dimensionally $[W] = [A_{21}/B_{21}] = ML^{-1}T^{-1}$, so that the energy can be scaled to $w = (B_{21}/A_{21})W$ and Eqs. (1)–(3) become

$$\frac{dn_1}{dt} = -\frac{n_1}{t_1} + n_2 + w(n_2 - n_1), \tag{17}$$

$$\frac{dn_2}{dt} = r - n_2 - w(n_2 - n_1), \tag{18}$$

$$\frac{dw}{dt} = \frac{(A'_{21}/A_{21})n_2 + w(n_2 - n_1)}{t_0(1 - t_1)} - \frac{w}{t_0}. \tag{19}$$

The ratio A'_{21}/A_{21} is calculated as follows. The spontaneous decay rate of all transitions between levels 2 and 1 is A_{21}, so that the spontaneous decay rate at frequency ν is

$A_{21}g(\nu)$. The standard result of radiation theory is that the number of possible modes of oscillation in a cavity volume V in unit frequency range is

$$N(\nu) = (8\pi\nu^3/c^3)V. \tag{20}$$

Therefore, the spontaneous emission rate into each mode is $A_{21}g(\nu)/N(\nu)$ and the spontaneous emission rate into the mode at the center of the Lorentzian ($\nu = \nu_0$) is

$$A'_{21} = A_{21}g(\nu_0)c^3/8\pi\nu_0^2 V. \tag{21}$$

Thus

$$\frac{A'_{21}}{A_{21}} = \frac{2}{A_{21} + T_1^{-1}} \frac{c^3}{8\pi\nu_0^2 V}. \tag{22}$$

The values of these variables for the specific laser being modeled can be substituted into this formula. As will be seen in Sec. V, A'_{21}/A_{21} is very small when realistic values are used for the parameters in (22). It is this that leads to the suspicion, unjustified in our experience, that the differential equations may be stiff and therefore require special treatment. Equations are stiff if their solutions contain time constants of greatly differing magnitude, such as can occur with a rapidly decaying transient solution.

Equations (17)–(19) are in a form that can easily be programmed for a computer, and as mentioned in Sec. I, a standard fourth-order Runge–Kutta subroutine can be used, with variable step length to select the appropriate integration interval.

V. COMPUTER EXPERIMENTS

The computational model offers many possibilities of numerical experiments which give insight into the theory and behavior of the laser. The experiment described here is an investigation into the time variation of the population levels and energy in the cavity after the initiation of pumping.

Before an experiment is performed, a suitable means of displaying the resulting data is required. For this project a laser printer with high-level graphics routines was available. This meant that the lists of numbers produced by the solution of the equations could be converted very simply into graphs showing the time variation of the variables. In general, graphical depiction of results is more easily digested than lists of numbers.

For the numerical simulation, values were chosen to give good illustration of laser action. Since the results are presented in dimensionless form, the qualitative features to be discussed are not dependent on the exact numerical values. We put

$$T_1 = 5\times10^{-8}\ \text{s}, \tag{23}$$

$$T_2 = A_{21}^{-1} = 10^{-7}\ \text{s}, \tag{24}$$

$$T_0 = 10^{-6}\ \text{s}. \tag{25}$$

The dimensionless time parameters are then $t_1 = T_1/T_2 = 0.5$ and $t_0 = T_0/T_2 = 10$. Substitution of the numerical values into (22) gives the dimensionless parameter $A'_{21}/A_{21} = 1.5\times10^{-8}$. The smallness of this number is physically very important, a point that will be enlarged on later.

Some numerical experiments on the start-up of the laser are shown in Fig. 4. The initial values of w, n_1, and n_2 are set at zero, and the equations are integrated with different pump rates. In Fig. 4(a), the pump rate is half the threshold value, and as expected, the energy in the lasing mode rises to a very low value. The emission in this case is due almost entirely to spontaneous transitions. The pump rates in Fig. 4(b) and 4(c) are greater than threshold, so that lasing can take place. The figures show that the lasing state is reached in two steps. First, on a time scale of order $T_2 = A_{21}^{-1}$, the spontaneous lifetime of the upper lasing level, the system switches to the unstable, nonlasing solu-

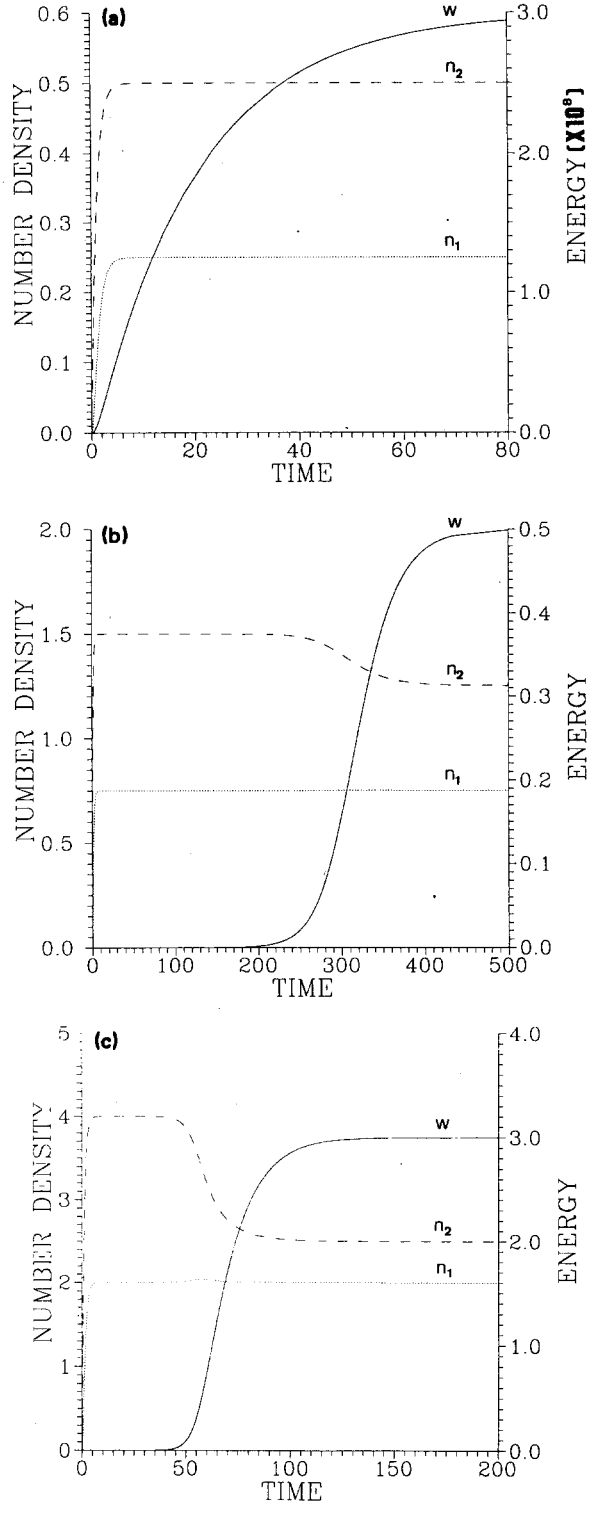

Fig. 4. Time evolution of occupation numbers n_1 and n_2 and laser energy w. Pump rate is increased from zero to r at time $t = 0$. Dimensionless variables are defined in text. (a) $r = 0.5$, (b) $r = 1.5$, and (c) $r = 4$.

tion given by (11). Second, on a much longer time scale, of order 10–100 times T_2, the system switches from the nonlasing to the stable lasing solution. During this process, the population density N_1 stays essentially constant, since according to (8) it is independent of W, while N_2 drops from its unstable to its stable value.

The reason for the occurrence of two very different time scales in the numerical solution is the smallness of the ratio A'_{21}/A_{21} in (22). This arises, it will be recalled, because A_{21} is the decay rate for transitions with photon emission into all the cavity modes within the line shape (Fig. 2), whereas A'_{21} is the rate for transitions with emission into the cavity mode that is actually lasing. In fact, in our first numerical simulations, we simply omitted the term A'_{21}; we than found that the system stays in the nonlasing state even though it is unstable and it might not have persisted in the presence of numerical rounding. Inclusion of the term A'_{21} is vital if the numerical solutions are to show a transition into the lasing state. Physically, it is the spontaneous emission into the lasing modes that provides the noise that is amplified, eventually switching the system from the nonlasing to the lasing state.

Comparison of Figs. 4(b) and 4(c) shows that, as might be expected, the transition to the lasing state takes place more rapidly at the higher pump rate.

Once the computer program has been developed, there are many other numerical experiments which could be carried out. Investigations into pulsed lasers is one possibility. One common method of producing short, intense laser pulses is Q switching. In this case, the laser oscillations are prevented in the cavity by reducing the Q of the cavity while pumping energy in, so that a high degree of population inversion is obtained. When the Q is switched to a high value, the energy in the laser builds up rapidly, converting the energy of the atoms into a short pulse of laser light. This can be modeled by setting the initial value of the population inversion ($N_2 - N_1$) to a high value before starting to integrate the rate equations. However, the present model is somewhat too simple to simulate this successfully, since the lifetime of the upper short-lived state (Fig. 2) has been neglected. If the time scale of the pulse is short compared to this lifetime, it needs to be taken into account. The equations can easily be expanded to include level 3.[6] It should also be possible to modify the model to produce unstable or chaotic solutions, which are of particular interest at the moment (for example, Lippi *et al.*)[7] Another area of interest in pulsed laser systems is relaxation oscillations, in which the laser energy builds up so rapidly that the population inversion is depleted. This causes a reduction in gain, thus allowing the inversion to build up again, and so on. The result is a series of short pulses of decreasing amplitude. The present model could be used to model such an effect, but since the effect are transient, it is likely that the time scales of the atomic lifetimes and the pulses differ greatly, producing stiff equations. As mentioned previously, such stiff equations would need a different subroutine for integration.

VI. CONCLUSIONS

It is hoped that this example of a mathematical model of laser action brings out a number of points about the teaching of computational physics at the undergraduate level.

First, the example should dispel any notion that "putting the equation through the computer" is somehow an automatic process that removes the need for analysis of the system based on good physical insight. In fact, it tends to support the converse view that numerical study demands and can help produce better insight. Thus the crucial role played by the spontaneous emission term in (3) in the transition to laser action emerges very clearly from the numerical work, and once it is perceived, a return to the original equations shows the reason.

Second, we would argue that it is helpful for the students to be taught some of the techniques of computational physics, and not simply left to pick them up some time in their later careers. The crucial part played by the steady-state solutions in the development of the computational analysis is not untypical of numerical work. We have found that the need for so much analytical work comes as a surprise to our students, and they often need help in analyzing the steady-state solutions. Likewise, the importance of working in sensibly defined reduced (generally dimensionless) variables is not at all self-evident to the beginner. The investigation of the steady-state solutions and the conversion of the rate equations to dimensionless form does demand some degree of mathematical sophistication, even though the algebraic steps are not difficult in themselves.

The existence of exact solutions for the steady state is also very helpful in checking the numerical work. It is, of course, quite easy to write a program that is syntactically correct but still contains errors, and it is a great advantage if exact solutions are available for some limiting or special case. The fact that the graphs of Figs 4(b) and 4(c) go from an unstable to a stable steady-state solution does not prove that the program is correct, but it is certainly very encouraging.

In practice, we believe this project is generally very instructive. The students were surprised by the analytic work required at the beginning, and mostly they find the steps involved unfamiliar and rather difficult. Given some help with this part, however, they display considerable proficiency in writing a program and getting it to run. As discussed in Sec. I, we believe this project to be quite typical of the computing that graduates are likely to meet later. In particular, programming using library subroutines is very common, and significant and useful computing skills are learned from this technique: reading subroutine documentation, understanding parameters and common blocks, and constructing user supplied subroutines. There is no doubt that when the project is successful the students gain substantial insight into the physics of laser operation; it appears to us that this is complementary to what they learn about computational methods.

In the development of a course on computational physics, it is necessary to make decisions about the balance between formal lectures and project, or laboratory, type work. We have leaned very much toward the latter, partly because of a belief that students would not see the relevance of too much detailed material on numerical analysis, and partly because we wish to exploit an obvious opportunity for learning from practical experience. Here, computational physics is paired with microprocessor instrumentation in an optional course that is intended to occupy one-fifth of the lecture time during the final year; opinion among the students is that the course is very time consuming, but can be worthwhile. In addition to some half-dozen lectures to give an appreciation of numerical analysis, the computational part comprises a short revision example to refresh programming knowledge, a numerical example to

give experience of some branch of mathematical software such as quadrature or root finding, and a project such as the one described here.

ACKNOWLEDGMENT

The authors would like to thank Professor R. Loudon for the help he has given throughout this project.

[a] Present address: Brunel University, Uxbridge, Middlesex UB8 3PH, UK.

[1] D. R. Tilley, "Physics and computing," Phys. Bull. **36**, 456–458 (1985).

[2] NAG FORTRAN library, Mark II (Numerical Algorithms Group Ltd., Gordon Hill Road, Oxford OX2 8DR, UK, 1983).

[3] W. H. Press, B. P. Flannery, S. A. Teukolsky, and W. T. Vetterling, *Numerical Recipes* (Cambridge U.P., New York, 1986).

[4] A. Yariv, *Optical Electronics* (Holt-Saunders, New York, 1985), 3rd ed., pp. 141–158.

[5] R. Loudon, *The Quantum Theory of Light* (Oxford U.P., Oxford, UK, 1983), 2nd ed., pp. 54–56.

[6] D. G. H. Andrews, "A numerical model of synchronously pumped mode-locked dye laser, based on the rate equations for three levels," Opt. Commun. **78**, 363–368 (1990).

[7] G. L. Lippi, N. B. Abraham, G. P. Puccioni, F. T. Arecchi, and J. R. Tredicce, "Evidence that transverse effects cause an instability in a single-mode CO_2 laser," Phys. Rev. A **35**, 3978–3981 (1987).

Laboratory studies of air flow visualization using holographic interferometry

K.-E. Peiponen and R. M. K. Hämäläinen
Väisälä Laboratory, Department of Physics, University of Joensuu, SF-80100, Finland

Toshimitsu Asakura
Research Institute of Applied Electricity, Hokkaido University, Sapporo, Hokkaido 060, Japan

(Received 16 November 1989; accepted for publication 14 November 1990)

Holographic interferometry was used to visualize a low-velocity cooled air flow. The physical properties of the heat exchange of the system were investigated using holographic interferometry.

I. INTRODUCTION

The visualization of the flow of a transparent gas has some problematic features. A conventional method generally employed in engineering applications is to visualize the gas flow with the aid of trace particles[1] so that the properties of the flow can be studied by defining the stream lines of the tracers. A problem that often arises with tracers is that they usually have different specific gravities from the flowing gas to be visualized. In this kind of situation, the stream lines of the tracers do not correspond to the true stream lines of the flow. Another problem with tracers occurs when we study transient flow, which may change quickly. Because of different specific gravities, the tracers may be unable to follow properly the quick change in the flow.

One solution may be provided by holographic interferometry, which has recently been investigated in the field of optical engineering. This provides a nondestructive method for investigating the gas flow without disturbing it. For flow diagnostics with the aid of holography, however, we need to produce a thermodynamical state of flow so that the refractive index of the gas changes strongly enough in the area of a jet field for it to be visualized.

At universities where elements of holography are taught, a common way of introducing the experimental procedures of holography to undergraduate students is to let them record holograms from a static object. To record a good-quality hologram, the object is usually chosen for its qualities as a good reflector in order to make the object wave interact properly with the reference wave on the film plate.

A more advanced stage in holographic experiments at universities may involve phase objects such as the flow of gas. In this case, the objects usually assume a dynamic nature. For students, it is quite fascinating, for example, to observe that something which is transparent can be made visible. In general, the physical properties of the gas flow are important, especially in the engineering field. Such properties may usually remain on an abstract level, but can be qualitatively, and to some extent also quantitatively, understood by studying the interferograms obtained in holographic intreferometry.

In this article, we briefly introduce some ideas on the problem of how to study the physics of a gas flow with the aid of holographic interferometry. Cooled air with relatively slow flow velocity is found applicable for studies of gas flow, since relatively simple thermo-optical properties of the system are involved.

II. FLOW VISUALIZATION

We studied the air flow through a nozzle. In Fig. 1 we show a typical nozzle of the present study. In Fig. 2 is presented an experimental arrangement for the holographic visualization of a steady, uniform, and nonchanging flow. The nonchanging flow was obtained using the Joensuu University air compressor system. The pressure difference between the stagnation chamber and the laboratory room was measured with a digital micromanometer. A cw He–Ne laser, which is most frequently available at universities, was used as the light source. The output beam of the laser is split by a beam splitter to reference and object waves. The diffuser, consisting of a ground-glass plate, makes the object wave spread uniformly on the object. Spatial filtering is also performed in the focal plane of the lenses by introducing a small aperture to eliminate the optical noise caused by dust particles. In this experiment a vi-